Vibration Suppression Control for a Flexible Beam with Sliding Mode Observer

Shibly Ahmed Al-Samarraie
University of Technology
Control & Systems Engineering
Department

Mohsin N. Hamzah
University of Technology
Mechanical Engineering
Department

Imad Abdulhussein Abdulsahib
University of Technology
Mechanical Engineering
Department

dr.shiblyahmed@yahoo.com   dr.mohsin@uotechnology.edu.iq   emad099@yahoo.com

Abstract

In this study, the vibration suppression of smart structure is performed by using piezoelectric patch structure. The smart structure consists of a beam, as a host structure, and piezoelectric patches, attached to the surface of the beam, as actuation and sensing elements. Two sources of instabilities, namely, the observer spillover and the control spillover, are considered in the current design of the controller based on a reduced order model of the large scale system.

To design a controller, that will attenuate the vibration, the balance realization is used to select the reduced order model that is most controllable and observable. Eight state is selected for the reduced model in the present work.

The sliding mode observer, which based on the equivalent control, is designed to estimate eight states of the reduced model where the state estimation error is proved bounded. By using the estimated state via sliding mode observer an optimal LQR controller is designed that attenuate the vibration of a smart cantilever beam using piezoelectric element. To overcome the control spillover problem, an avoidance condition was derive, that will ensure the asymptotic stability for the proposed vibration control design.

The numerical simulations are preformed to test the vibration attenuation ability of the proposed optimal control. For 10 mm initial tip displacement, the piezoelectric actuator found able to reduce the tip displacement to about 1.3 mm after 15s, while it equal to 7 mm with the open loop case.

The simulations show, also, that the optimal control action is performed with minimum effort where only 30 voltage is required while piezoelectric actuator is saturated at 200 voltage.

1. Introduction

Vibration control of flexible structures is of great interest, as light structures in all engineering applications are getting much more important. One way of making the structure as smart one is done by the use of piezoelectric materials. These smart materials can be used as sensors and actuators, they are flexible enough to be placed in a variety of places and have the capacity to work in high frequency ranges [1]. The system is called a smart structure because it has the ability to perform self-controlling. The technology of smart structures, of those with piezoelectric patches, have received much attention in recent years, because piezoelectric materials have simple mechanical properties, small volume, light weight, efficient conversion between electrical and mechanical energy, and good ability to perform vibration control [2]. One of the application of piezoelectric smart structures is the control and suppression of unwanted structural vibrations [3]. The electricity for the piezoelectric is produced by pressure (Direct Effect). Conversely, a piezoelectric material deforms when it is subjected to an electric field (Converse Effect). The piezoelectric sensor senses the external disturbances and generates voltage due to direct piezoelectric effect while piezoelectric actuator produces force due to converse piezoelectric effect which can be used as controlling force [4].

Mechanical structures are systems with continuous, distributed parameter. To simulate their behavior under inertia and external loads, very few analytical solutions for specific situations are available. For this reason, the discretization of these structures is the basic step for a static and dynamic further analysis. One possibility for this step is provided by the Finite Element (FE) Method. In mathematical terms, Finite Elements are a numerical method for solving systems, which generally used to eliminate all spatial derivatives by increasing, at the same time, the number of the resulting new equations in the system [5].

In the finite element modeling, the structure is modeled to retain large number of degrees of freedoms. In active vibration control, the use of smaller order model has computational advantages. Therefore, it is necessary to apply a model reduction techniques in order to get a reduced model size for which the the control law can be designed. One of these techneques is based on balance realization method [6]. The approach taken for reduction the order of a given model based on removal the coordinates, that are the

least controllable and observable. To implement this idea, a measure of the degree of controllability and observability is required [7].

For closed-loop system, it is not always possible to get a control law that cause eigenvalues to have the required and desired values. This problem raises the concept of controllability. The system is completely controllable if every state variable can be affected in such a way as to cause it to reach a particular value within a finite amount of time by some unbounded control. However, an alternative, more useful measure is provided for asymptotically stable systems of the form given by equations by defining the controllability gramian. Gramian matrices can be used for checking if a system is controllable and observable [8].

To control vibration of a piezoelectric smart structure, a controller usually designed based on a reduced order model (ROM) of the system form, whereas, FE models inevitably have a large number of degrees of freedom. When such a ROM based controller is applied to the full order system, actuator forces for reducing the vibration of the lower modes will also influence the residual modes of the structure and produce undesirable vibration due to the un-modeled dynamics. This phenomenon is known as control spillover [9]. Spillover phenomenon occurs because the unmodeled dynamics, which are not included in reduce order model, will be excited.

Similarly, the sensor will sense the deflection not only from the lower modes but also from the other modes, giving rise to the so-called observation spillover. Spillover effects are undesirable and may cause performance degradation and even system instability [10]. In fact, the only way to avoid a spillover that comes from the state estimation or observation process is to use an observer that will estimate the states with minimal error.

Various control strategies have been suggest and applied to different flexible systems in order to suppress vibration of flexible structures. Some of these studies are feedback control, linear quadratic regulator (LQR) approach [11], H_2 control, H_∞ control [12] and sliding mode control [13]. The theory of optimal control is concerned with operating a dynamic system at minimum cost. The case where the system dynamics are described by a set of linear differential equations and the cost is described by a quadratic function is called the LQ problem. The linear-quadratic regulator provides one of the main results in the theory. The settings of a (regulating) controller governing either a machine or process are found by using a mathematical algorithm that minimizes a cost function with weighting factors. The cost function is often defined as a sum of the deviations of key measurements from their

desired values. Often the magnitude of the control action itself is included in this sum so as to keep the energy spent by the control action itself limited [11]. The LQR is the most commonly used controller in smart structures [14-17].

The controller requires state measurement; an observer is designed to estimate the states. Observers are dynamic systems that can be used to estimate the unavailable state variables of a plant. Luenberger observer [18], is the most famous that used a dynamical linear system to generate estimates of the plant states. In some cases, the inputs are unknown or which led to the development of the unknown input observer. For the smart beam, which modeled by a finite elements with a reduced number of states, the remaining states which are acting on the reduced model will be regarded as unknown inputs.

Many researcher interested with the sliding mode observer design for uncertain dynamical systems; several observers design are given by Utkin [19], Walcott, et al [20], Zak, et al [21], Edwards and Spurgeon [22], and Slotine, et al [23]. Despite the robustness property to the sliding mode observer, the present of unknown inputs (the remaining states) that do not satisfy matching condition will definitely cause error in the estimation process. The main advantage of using sliding-mode observers is that, while in sliding, they are insensitive to the matched unknown inputs. Moreover, they can be used to reconstruct unknown inputs, which could be a combination of system disturbances [24].

The aim of the present paper is to design an optimal LQR controller based on sliding mode observer to attenuate the vibration of a smart cantilever beam using piezoelectric element. The model utilized for control design purpose is the reduced order model that is obtained according to the balance realization method. Based on the equivalent control, the SMO is designed to minimize the estimation error which it is a basic requirement to avoid observer spillover danger. Moreover the control spillover is eliminated in our proposed vibration suppression control design via deriving the avoidance condition.

2. Modeling of Smart Cantilever Beam Using Euler Bernoulli Beam Theory

The model of clamped-free flexible beam studied here is given in Fig.1. The cantilever beam bonded with collocated piezoelectric sensor/ actuator pair at the free end. The piezoelectric material is the Lead-Zirconate-Titanate (PZT) which it is the most popular piezoelectric materials. By using the Euler-Bernoulli beam equation, the infinite dimensional mathematical expression of the beam can be written as follows [25];

$$c^2 \frac{\partial^4 w(x,t)}{\partial x^4} + \frac{\partial^2 w(x,t)}{\partial x^2} = 0 \qquad \text{.... (1)}$$

Where $c^2 = EI/\rho A$, $w(x,t)$ is the deflection along the x-axis, E is the Young's modulus, I is the moment of inertia, A is the cross sectional area, and ρ is the density of the beam. The partial differential equation (PDE) given by Eq. (1) can be solved by using the assumed mode approach, which yields finite dimensional ordinary differential equation set.

The dynamic equation of the smart structure is obtained by using both regular beam element and piezoelectric beam elements. The mass and stiffness matrices of the smart structure include sensor/actuator mass and stiffness [26]. The entire structure is modelled in state space form using the Finite Element Method (FEM) by dividing the structure into four equal finite elements. The sensor and actuator were integrated on the top and bottom surfaces of the end element of the beam. A beam element is considered with two nodes at its end. Each node is having two degree of freedom (DOF) (translation and rotation) is considered. The function that will describe the element translational and rotational state at each point is named as the shape function of the element which are derived by applying boundary conditions. The mass and stiffness matrix is derived using shape functions for the beam element. When a system vibrates, it undergoes back and forth motion, it has transverse displacements, so all positions vary with time, and therefore, the system has velocities and accelerations. Mass times acceleration as inertia force appears in the governing differential equation of the beam, which is given in Eq. (1), the equation of motion, involves a fourth order derivative w.r.t. x, and a second order derivative w.r.t. time (acceleration). The solution of the Eq. (1) is assumed as a cubic polynomial function of x given by:

$$w(x) = a_1 + a_2 x + a_3 x^2 + a_4 x^3 \qquad \text{... (2)}$$

Where $w(x)$ is displacement function which satisfies the fourth order partial differential equation, Eq. (1). The constants a_1 to a_4 be obtained by using the boundary conditions at both the nodal points (fixed end and free end). The mass matrix, as derived in Appendix A, is

$$M_b = \rho_b A_b \int_{l_b} N N^T dx =$$
$$\frac{\rho_b A_b l_b}{420} \begin{bmatrix} 156 & 22l_b & 54 & -13l_b \\ 22l_b & 4l_b^2 & 13l_b & -3l_b^2 \\ 54 & 13l_b & 156 & -22l_b \\ -13l_b & -3l_b^2 & -22l_b & 4l_b^2 \end{bmatrix} \quad \text{... (3)}$$

Where M_b is the mass matrix of regular beam, N is the shape function and l_b is the length of the regular beam, ρ_b is the mass density of the beam

material, A_b is the cross sectional area of the beam, I_b is the moment of inertia of the beam, and E_b is the modulus of elasticity of the beam material.

Also from Appendix A, the stiffness matrix is obtained in the following form

$$K_b = E_b I_b \int_{l_b} N_2 N_2^T \, dx =$$
$$\frac{E_b I_b}{l_b^3} \begin{bmatrix} 12 & 6l_b & -12 & 6l_b \\ 6l_b & 4l_b^2 & -6l_b & 2l_b^2 \\ -12 & -6l_b & 12 & -6l_b \\ 6l_b & 2l_b^2 & -6l_b & 4l_b^2 \end{bmatrix} \quad \text{... (4)}$$

Where K_b is the stiffeness matrix of regular beam, N_2 is the second derivative of the shape function N.

Eventually the equation of motion according to the Lagrangian equation is:

$$M_b \ddot{q} + K_b q = f_b \qquad \text{.... (5)}$$

Or

$$\frac{\rho_b A_b}{420} \begin{bmatrix} 156 & 22l_b & 54 & -13l_b \\ 22l_b & 4l_b^2 & 13l_b & -3l_b^2 \\ 54 & 13l_b & 156 & -22l_b \\ -13l_b & -3l_b^2 & -22l_b & 4l_b^2 \end{bmatrix} \begin{bmatrix} \ddot{w}_1 \\ \ddot{\theta}_1 \\ \ddot{w}_2 \\ \ddot{\theta}_2 \end{bmatrix} +$$

$$\frac{E_b I_b}{l_b^3} \begin{bmatrix} 12 & 6l_b & -12 & 6l_b \\ 6l_b & 4l_b^2 & -6l_b & 2l_b^2 \\ -12 & -6l_b & 12 & -6l_b \\ 6l_b & 2l_b^2 & -6l_b & 4l_b^2 \end{bmatrix} \begin{bmatrix} w_1 \\ \theta_1 \\ w_2 \\ \theta_2 \end{bmatrix} = \begin{bmatrix} F_1 \\ M_1 \\ F_2 \\ M_2 \end{bmatrix}$$
$$\text{.... (6)}$$

Where F_1 , F_2, M_1, M_2 are the forces and the bending moments acting on nodes 1 and 2 respectively (Fig. (1)). and q is the displacements at the nodes, $q = [w_1\ \theta_1\ w_2\ \theta_2]^T$, w_1, θ_1, w_2 and θ_2 are Degree of Freedom at node 1 and 2, respectively.

When PZT patches are assumed as Euler-Bernoulli beam elements the elemental mass and stiffness matrices of PZT beam element can be computed in similar fashion as [25]:

$$M_p = \frac{\rho_p A_p l_p}{420} \begin{bmatrix} 156 & 22l_p & 54 & -13l_p \\ 22l_p & 4l_p^2 & 13l_p & -3l_p^2 \\ 54 & 13l_p & 156 & -22l_p \\ -13l_p & -3l_p^2 & -22l_p & 4l_p^2 \end{bmatrix}$$
$$\text{.... (7)}$$

$$K_p = \frac{E_p I_p}{l_p^3} \begin{bmatrix} 12 & 6l_p & -12 & 6l_p \\ 6l_p & 4l_p^2 & -6l_p & 2l_p^2 \\ -12 & -6l_p & 12 & -6l_p \\ 6l_p & 2l_p^2 & -6l_p & 4l_p^2 \end{bmatrix} \quad \text{... (8)}$$

The smart beam element is obtained by sandwiching the regular beam element in between the two PZT patches (Fig. 1).
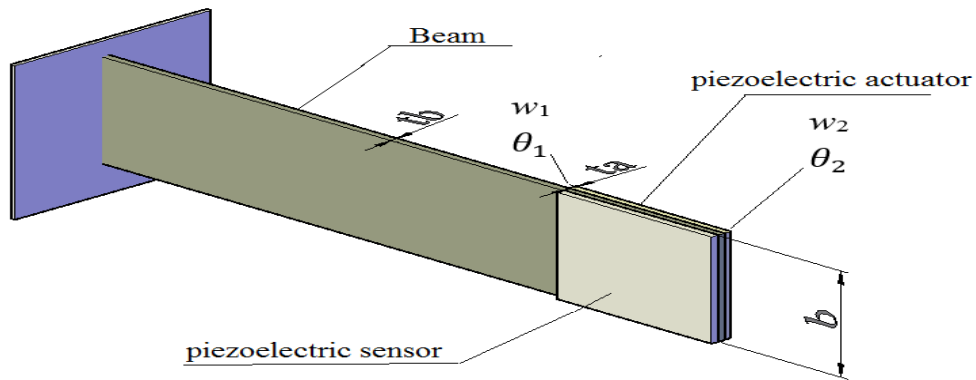
Figure 1: Clamped-free flexible smart beam model

In which $EI = E_b I_b + 2E_p I_p$ is the flexural rigidity and $\rho A = b(\rho_b t_b + 2\rho_p t_p)$ is the mass per unit length of smart beam element, t_p is the thickness of PZT patches thickness of Actuator and Sensor, and $I_p = \frac{b t_a^3}{12} + bt_a \left(\frac{t_a+t_b}{2}\right)^2$. So the elemental mass and stiffness matrices of smart beam element are:

$$M = \frac{\rho A l_p}{420} \begin{bmatrix} 156 & 22l_p & 54 & -13l_p \\ 22l_p & 4l_p^2 & 13l_p & -3l_p^2 \\ 54 & 13l_p & 156 & -22l_p \\ -13l_p & -3l_p^2 & -22l_p & 4l_p^2 \end{bmatrix}$$

$$.... (9)$$

$$K = \frac{EI}{l_p^3} \begin{bmatrix} 12 & 6l_p & -12 & 6l_p \\ 6l_p & 4l_p^2 & -6l_p & 2l_p^2 \\ -12 & -6l_p & 12 & -6l_p \\ 6l_p & 2l_p^2 & -6l_p & 4l_p^2 \end{bmatrix} \quad .... (10)$$

2.1 Sensor and Actuator Equations

The sensor equation is derived from the direct piezoelectric equation, which is used to calculate the total charge created by the strain in the structure. Piezoelectric materials can be used as strain rate sensors. When used so, the output charge can be transformed into the sensor current $i(t)$ [23]:

$$i(t) = z\, e_{31}\, b \int_{x_i}^{x_i+l_b} N_2^T \dot{q}\, dx \qquad .... (11)$$

Where, $z = \frac{t_b}{2} + t_a$ and N_2 is the second spatial derivative of the shape function, e_{31} is the piezoelectric stress constant.

The output current of the piezoelectric sensor measures the moment rate of the flexible beam. This current is converted into the open circuit sensor voltage $V_s(t)$ using a signal-conditioning device with the gain G_c. Thus [25]:

$$V_s(t) = \begin{bmatrix} 0 & -G_c z\, e_{31}\, b & 0 & G_c z\, e_{31}\, b \end{bmatrix} \begin{bmatrix} \dot{w}_1 \\ \dot{\theta}_1 \\ \dot{w}_2 \\ \dot{\theta}_2 \end{bmatrix}$$

$$= Sc \begin{bmatrix} 0 & -1 & 0 & 1 \end{bmatrix} \begin{bmatrix} \dot{w}_1 \\ \dot{\theta}_1 \\ \dot{w}_2 \\ \dot{\theta}_2 \end{bmatrix} = p^T \dot{q} \quad .... (12)$$

Where $S_c = G_c z\, e_{31}\, b$ and p is a constant vector depends on the type of sensor, its characteristics and its location on the beam.

The actuator equation is derived from the converse piezoelectric equation. The strain developed ϵ_x by the electric field E_f on the actuator layer is given by [27]:

$$\epsilon = dE_f \qquad .... (13)$$

Where, $E_f = \frac{V_a(t)}{t_a}$ is the electric field, and $V_a(t)$ is the input voltage applied to the piezoelectric actuator in the thickness direction t_a. Then the stress σ_a that developed by the actuator is given by: [25]

$$\sigma_a = E_p d_{31} \left(\frac{V_a(t)}{t_a}\right) \qquad .... (14)$$

Where E_p is the Young's modulus of the piezoelectric and d_{31} is piezoelectric strain constant.

The bending moment in a small cross section of the piezoelectric element is given by:

$$dM_a = E_p I_p \frac{d^2 w}{dx^2} \qquad .... (15)$$

The resultant moment M_a acting on the beam element due to the applied voltage V_a is determined by integrating the stress in Eq. (14) throughout the structure thickness as:

$$M_a = E_p d_{31} z\, V_a(t) \qquad .... (16)$$

The control force f_{ctrl} produced by the actuator that is applied on the beam element is obtained as [25]:

$$f_{ctrl} = E_p d_{31} b \, z \, [-1 \ 0 \ 1 \ 0]^T V_a(t) \qquad .... (17)$$

Alternatively, f_{ctrl} can be expressed as:

$$f_{ctrl} = h \, V_a(t) \qquad .... (18)$$

where,
$$h = E_p \, d_{31} \, b \, z \, [-1 \ 0 \ 1 \ 0]^T \qquad .... (19)$$

3. Dynamic Equation of Smart Structure

The dynamic equation of the smart structure is obtained by using both the regular and piezoelectric beam elements (local matrices) given by Eq. (9) and Eq. (10). The mass and stiffness of the bonding or the adhesive between the master structure and the sensor / actuator pair is neglected. The mass and stiffness of the entire beam, which is divided into four finite elements with the piezo-patches placed at only one discrete location is assembled using the FEM technique and the assembled matrices (global matrices) M and K are obtained. The equation of motion of the smart structure is given by: [25]

$$M \, \ddot{q} + Kq = f_{ext} + f_{ctrl} = f \qquad ... (20)$$

where M, K, f_{ext}, f_{ctrl} and f are the global mass matrix, global stiffness matrix of the smart beam, the external force applied to the beam, the controlling force from the actuator and the total force coefficient vector respectively.

The generalized structural modal damping matrix D is introduced into Eq. (20) by using: [28, 29]

$$D = \alpha M + \beta K \qquad .... (21)$$

where α and β are the frictional damping constant and the structural damping constant respectively. When applying the cantilever beam boundary condition, the system equation of motion for the 4-element cantilever beam is:

$$M \, \ddot{q} + D\dot{q} + Kq = f \qquad .... (22)$$

For free vibration condition f_{ext} equal to zero, so the remaining applied force on the system is the controlling force f_{ctrl} exerted by the controller.

3.1 State Space Model of the Smart Beam

Many design tools and model reduction in modern control theory need a state space form for the mathematical model of a plant. Consequently, the smart flexible cantilever beam mathematical model can be written in state space form as follows;

Let $\quad q = \begin{bmatrix} q_1 \\ q_2 \end{bmatrix} = \begin{bmatrix} x_1 \\ x_2 \end{bmatrix} = x$, $\dot{q} = \begin{bmatrix} \dot{q}_1 \\ \dot{q}_2 \end{bmatrix} = \begin{bmatrix} \dot{x}_1 \\ \dot{x}_2 \end{bmatrix} = \begin{bmatrix} x_3 \\ x_4 \end{bmatrix}$,

and $\quad \ddot{q} = \begin{bmatrix} \dot{x}_3 \\ \dot{x}_4 \end{bmatrix}$ then the 4-element smart cvantilever beam sate space model is;

$$M \begin{bmatrix} \dot{x}_3 \\ \dot{x}_4 \end{bmatrix} + D \begin{bmatrix} x_3 \\ x_4 \end{bmatrix} + K \begin{bmatrix} x_1 \\ x_2 \end{bmatrix} = f_{ctrl} \qquad ... (23)$$

which yields to

$$\begin{bmatrix} \dot{x}_3 \\ \dot{x}_4 \end{bmatrix} = -M^{-1}D \begin{bmatrix} x_3 \\ x_4 \end{bmatrix} - M^{-1}K \begin{bmatrix} x_1 \\ x_2 \end{bmatrix} + M^{-1}h \, V_a(t) \qquad .... (24)$$

Or

$$\begin{bmatrix} \dot{x}_1 \\ \dot{x}_2 \\ \dot{x}_3 \\ \dot{x}_4 \end{bmatrix} = \begin{bmatrix} 0 & I \\ -M^{-1}K & -M^{-1}D \end{bmatrix} \begin{bmatrix} x_1 \\ x_2 \\ x_3 \\ x_4 \end{bmatrix} + \begin{bmatrix} 0 \\ M^{-1}h \end{bmatrix} u(t) \qquad .... (25)$$

And in a matrix form

$$\dot{x} = Ax(t) + Bu(t) \qquad .... (26)$$
Where

$$u(t) = V_a(t).$$

With approperate zero and identity matrices dimensions. The sensor voltage is taken as the output of the system and the output equation is obtained as:

$$y(t) = V_s(t) = p^T \dot{q} = p^T \begin{bmatrix} x_3 \\ x_4 \end{bmatrix} \qquad .... (27)$$

Thus, the sensor output equation in state space form is given by:

$$y(t) = [0 \quad p^T] \begin{bmatrix} x_1 \\ x_2 \\ x_3 \\ x_4 \end{bmatrix} \qquad .... (28)$$

Or,

$$y(t) = Cx(t) \qquad .... (29)$$

where $C = [0 \quad p^T]$. The single input single output state space model (state equation and the output equation) of the smart structure developed for the system is given by Eqs. (26) and (29):

$$\left. \begin{matrix} \dot{x} = Ax(t) + Bu(t) \\ y = Cx(t) \end{matrix} \right\} \qquad .... (30)$$

with

$$\left. \begin{matrix} A = \begin{bmatrix} 0 & I \\ -M^{-1}K & -M^{-1}D \end{bmatrix}_{16*16} \\ B = \begin{bmatrix} 0 \\ M^{-1}h \end{bmatrix}_{16*1} \\ C = [0 \quad p^T]_{1*16} \end{matrix} \right\} \qquad ... (31)$$

In the following section, the state space model is reduced via balance realization to a form and dimension more appropriate for controller and observer design.

3.2 Model Reduction

In the finite element modeling, the structure is modeled to retain large number of degrees of freedoms. In active vibration control, the use of smaller order model has computational advantages. Therefore, it is necessary to apply a model reduction technique to the state space representation. The reduced order system model extraction techniques solve the problem of the complexity by keeping the essential properties of the full model only [6]. For the present work the 16th order system model obtained from the finite element model is reduced to the 8th order using a model reduction technique based on balance realization.

The approach taken for reduction the order of a given model based on deleting the coordinates, or modes, that are the least controllable and observable. To implement this idea, a measure of the degree of controllability and observability is needed. However, an alternative, more useful measure is provided for asymptotically stable systems of the form given by equations by defining the controllability grammian, denoted by W_C, as [6] :

$$W_C^2 = \int_0^\infty e^{At} BB^T e^{A^T t} dt \qquad \dots (32)$$

And the observability grammian, denoted by W_O, as [6]:

$$W_O^2 = \int_0^\infty e^{A^T t} C^T C e^{At} dt \qquad \dots (33)$$

The matrices A, B, and C defined as in Eq. (31). The properties of these matrices provide useful information about the controllability and observability of the closed-loop system. If the system is controllable (or observable), the matrix W_C (or W_O) is nonsingular [30]. These grammians characterize the degree of controllability and observability by quantifying just how far away from being singular the matrices W_C and W_O are [31].

Applying the idea of singular values as a measure of rank deficiency to the controllability and observability grammians yields a systematic model reduction method. The matrices W_C and W_O are symmetric and hence are similar to a diagonal matrix. There is equivalent system for which these two grammians are both equal and diagonal. Such a system is called balanced system, also W_C and W_O must satisfy the two Liapunov-type equations:

$$\left. \begin{array}{l} A W_C^2 + W_C^2 A^T = -BB^T \\ A^T W_O^2 + W_O^2 A = -C^T C \end{array} \right\} \qquad \dots (34)$$

Now to transform the system to a balance realization form, this requires the determination of a transformation matrix P that will transform the system in Eq. (30) to:

$$\left. \begin{array}{l} \dot{x}' = A'x' + B'u \\ y = C'x' + Du \end{array} \right\} \qquad \dots (35)$$

where $A' = P^{-1}AP$, $B' = P^{-1}B$ and $C' = CP$. The controllability and observability grammians matrices are diagonal and equal

$$\widehat{W}_C = \widehat{W}_O = \Sigma = diag(\sigma_1, \sigma_2, \dots \dots, \sigma_n)$$

where $\widehat{W}_C$ and $\widehat{W}_O$ are the controllability and observability grammians for system after applying the transformation P and the numbers σ_i are the singular values of the grammians and are ordered such that

$$\sigma_i > \sigma_{i+1}, i = 1, 2, \dots \dots, n$$

Therefore the pair (A', B') could be uncontrollable pair since some of σ_j could be equal to zero. Indeed there exist a subsystem (i.e., a reduced order model) which is still controllable and observable.

Now the choice

$$P = G^{-1} U \Sigma^{\frac{1}{2}} \qquad \dots (36)$$

will transform the grammians W_C^2 and W_O^2 to become equal and transform the system in Eq. (30) to a balanced realization form. Namely,

$$\widehat{W}_C = \widehat{W}_o = \Sigma \qquad \dots (37)$$

where Σ can be written in terms of two set of the singular values $\sigma_{(1)}$ and $\sigma_{(2)}$ as

$$\Sigma = \begin{bmatrix} \sigma_{(1)} & 0 \\ 0 & \sigma_{(2)} \end{bmatrix} \qquad \dots (38)$$

In this representation $\sigma_{(1)}$ describes the "strong" sub-systems to be retained and $\sigma_{(2)}$ the "weak" sub-systems to be deleted. Conformally partitioning the matrices as

$$\left. \begin{array}{l} A' = \begin{bmatrix} A_{11} & A_{12} \\ A_{21} & A_{22} \end{bmatrix} \\ B' = \begin{bmatrix} B_1 \\ B_2 \end{bmatrix} \\ C' = \begin{bmatrix} C_1 & C_2 \end{bmatrix} \end{array} \right\} \qquad \dots (39)$$

and truncating the model, retaining $A_{1r} = A_{11}$, $B_r = B_1$ and $C_r = C_1$ as the reduced system, and deleting the "weak" internal subsystems [6].

4. LQR State Feedback Control Design

This section is devoted to design a linear state feedback controller to the reduced order model of the smart cantilever beam using Linear Quadratic Regulator (LQR). The LQR is an optimal control approach where the main objective of optimal control is to determine control signals that will cause a process to satisfy some physical constraints and at the same time (maximize or minimize) a chosen performance index or cost function [11]. To design an LQR control to the reduced order model of the smart beam the Reduced Model (RM) and the Residual Model (RSM) [9] are presented here as follows; according to the balance realization the linear state model for the cantilever beam, as given in Eq. (35) are rewritten as follow;

$$\left.\begin{array}{l}\dot{x}_r = A_{1r}x_r + A_{1R}x_R + B_1u \\ \dot{x}_R = A_{2r}x_r + A_{2R}x_R + B_2u \\ y = C_r x_r + C_R x_R\end{array}\right\} \quad \dots \text{(40)}$$

where $x_r \in \mathcal{R}^r$, is the reduced model states, $x_R \in \mathcal{R}^{n-r}$ is the residual model states, and

$$A = \begin{bmatrix} A_{1r}^{r\times r} & A_{1R}^{r\times(n-r)} \\ A_{2r}^{(n-r)\times r} & A_{2R}^{(n-r)\times(n-r)} \end{bmatrix},$$

$$B = \begin{bmatrix} B_1^{r\times 1} \\ B_2^{(n-r)\times 1} \end{bmatrix},$$

$$C = \begin{bmatrix} C_r^{1\times r} & C_R^{1\times(n-r)} \end{bmatrix}$$

The pair (A_{1r}, B_1) is the controllable pair and (A_{1r}, C_r) is the observable pair with highest controllability and observability grammian. From Eq. (40), the reduced model of the transformed model, which given in Eq. (35), is

$$\dot{x}_r = A_{1r}x_r + B_1u \quad \dots \text{(41)}$$

In the second step the performance index, J, is defined for the linear regulator problem as [6];

$$J = \frac{1}{2}\int_t^\infty (x_r^T Q\, x_r + u^T R\, u)\, dt, \quad \dots \text{(42)}$$

where Q and R are symmetric positive definite weighting matrices. The larger the matrix Q, the more emphasis is placed by optimal control on returning the system to zero, since the value of x corresponding to the minimum of the quadratic form $x_r^T Q\, x_r$ is $x = 0$. On the other hand, increasing R has the effect of reducing the amount, or magnitude, of the control effort allowed [6].

The optiumal control law that will minimize J is given by [32].

$$u(t) = -R^{-1} B_1 Px(t) = -K(t)x(t) \quad \dots \text{(43)}$$

where P is the solution to the algebraic Riccati Equation [32].

$$Q(t) - PB_1 R^{-1} B_1^T P + A_{1r}^T P + PA_{1r} = 0 \quad \text{(44)}$$

The linear controller, as in Eq. (43), that grantted asymptotic stabilty of the reduce model, may also cause the unstability for the system dynamic which named the control spillover. To avoid control spillover the avidness condition is derived below with a brief presentation of the spillover problem.

4.1 Control Spillover Problem and Avoidance Condition

To control vibration of a smart structure, a controller is usually designed based on a reduced order model of the system. When such a reduce order model based controller, is applied to the full order system, actuater force for reducing the vibration of the lower modes will also influence the residual modes of the structure and produce undesirable vibration due to the unmodeled dynamics. This phenomenon is known as control spillover [9]. Spillover phenomenon occurs because the unmodeled dynamics, which are not included in reduce order model, will be excited. In order to avoid the control spillover, an avoidnace condition is derived as follows; let the matrix Δ be defined as;

$$\Delta = \begin{bmatrix} (A_{1r} - B_1K) & A_{1R} \\ (A_{2r} - B_2K) & A_{2R} \end{bmatrix} \quad \text{(45)}$$

which represent the whole model matrix after applying the proposed LQR control. In order to avoid control spillover the matrix Δ must be Hurwitz with its minimum absolute real eigenvalue is larger than the absolute real eigenvalue of the matrix A (Eq. (30)). Namely, if R_i^C represent the real term to eigenvalue of Δ and R_i^O represent the real term to eigenvalue of A then the avoidance condition is;

$$R^C = \min_{i=1\to n}|R_i^C| > \min_{i=1\to n}|R_i^O| = R^O$$

For a large difference between R^C and R^O the vibration is attenuated effectively since the eigenvalue placed at R^O is the dominant one which shaped the cantilever beam response.

5. Sliding Mode Observer

For a large scale system, like the vibration control problem, the control spillover is not the only source for instability. There is another source of instability comes from imperfect or unprecise estimation for the states that are required for feeding back in the control law [13]. In fact the only way to avoid spillover that comes from the state estimation or observation process is to use an observer that estimates the states with minimal error. In the present work the Sliding Mode Observer (SMO) is used to estimate the states which it required in the control law (Eq. (43)).

The main advantage of using sliding model observer is that when the observer is in sliding mode, it is able to ensure that the difference between the system and observer outputs convergence to zero in finite-time even in the presence of the unknown inputs. Moreover, the SMO can be used also to reconstruct unknown inputs using equivalent control method [33]. By unknown input, we mean the residual term $(A_{1R}x_R)$ for the x_r dynamics (Eq. (40)) and the corresponding reduced order model in Eq. (41).

The general procedure for designing a sliding model observer for a linear system with unknown input are derived in the present work. For the linear time invariant system; (Eq (40))

$$\begin{rcases} \dot{x}_r = A_{1r}x_r + B_1u + D\xi \\ y = C_rx_r \end{rcases} \quad \dots (46)$$

where the unknown input $\xi = x_R \in \mathcal{R}^{n-r}$ and $D = A_{1R} \in \mathcal{R}^{r \times n-r}$. Now decompose x_r to $x_r = [x_1 \quad x_2]^T$ and C_r to $C_r = [C_1 \quad C_2]$, then the output y is:

$$y = C_rx_r = C_1x_1 + C_2x_2 \quad \dots (47)$$

where $x_1 \in \mathcal{R}^{r-1}$, $x_2 \in \mathcal{R}^1, C_1 \in \mathcal{R}^{1 \times (r-1)}$ $C_2 \in \mathcal{R}^1$ and $\det(C_2) \neq 0$. Accordingly Eq. (46), in terms of x_1 and x_2, can be written as

$$\begin{rcases} \dot{x}_1 = A_{11}x_1 + A_{12}x_2 + B_1u + D_1\xi \\ \dot{x}_2 = A_{21}x_1 + A_{22}x_2 + B_2u + D_2\xi \end{rcases} \quad \dots (48)$$

where $B_1 \in \mathcal{R}^{(r-1) \times 1}$, $B_2 \in \mathcal{R}^1$, $D_1 \in \mathcal{R}^{(r-1) \times n-r}$ and $D_2 \in \mathcal{R}^{1 \times n-r}$. Equation (48) can be written in terms of x_1 and y as follows;

$$\begin{rcases} \dot{x}_1 = \tilde{A}_{11}x_1 + \tilde{A}_{12}y + \tilde{B}_1u + \tilde{D}_1\xi \\ \dot{y} = \tilde{A}_{21}x_1 + \tilde{A}_{22}y + \tilde{B}_2u + \tilde{D}_2\xi \end{rcases} \quad \dots (49)$$

where x_2 is replaced by,

$$x_2 = C_2^{-1}(y - C_1x_1) \quad \dots (50)$$

And,

$\tilde{A}_{11} = A_{11} - A_{12}C_2^{-1}C_1$, $\tilde{A}_{12} = A_{12}C_2^{-1}$,
$\tilde{A}_{21} = C_1A_{11} + C_2A_{21} - (C_1A_{12} + C_2A_{22})C_2^{-1}C_1$
$\tilde{A}_{22} = (C_1A_{12} + C_2A_{22})C_2^{-1}$
$\tilde{B}_1 = B_1$, $\tilde{B}_2 = C_1B_1 + C_2B_2$
$\tilde{D}_1 = D_1$,, $\tilde{D}_2 = C_1D_1 + C_2D_2$,
Since $|C_2| \neq 0$, the transformation matrix between (x_1, x_2) and (x_1, y),

$$\begin{bmatrix} x_1 \\ y \end{bmatrix} = T_1 \begin{bmatrix} x_1 \\ x_2 \end{bmatrix} = \begin{bmatrix} I_{(r-1)} & O_{(r-1) \times 1} \\ C_1 & C_2 \end{bmatrix} \begin{bmatrix} x_1 \\ x_2 \end{bmatrix} \quad \dots(51)$$

is nonsingular.

To this end the proposed SMO to the system dynamic model as given in Eq. (49), is as follows;

$$\begin{rcases} \dot{\hat{x}}_1 = \tilde{A}_{11}\hat{x}_1 + \tilde{A}_{12}\hat{y} + \tilde{B}_1u - Lv \\ \dot{\hat{y}} = \tilde{A}_{21}\hat{x}_1 + \tilde{A}_{22}\hat{y} + \tilde{B}_2u - v \end{rcases} \quad \dots (52)$$

The error dynamics between the observer (Eq. (52)) and the system (Eq. (49)) is governed by

$$\begin{rcases} \dot{e}_1 = \tilde{A}_{11}e_1 + \tilde{A}_{12}e_y - Lv - \tilde{D}_1\xi \\ \dot{e}_y = \tilde{A}_{21}e_1 + \tilde{A}_{22}e_y - v - \tilde{D}_2\xi \end{rcases} \quad \dots (53)$$

where $e_1 = \hat{x}_1 - x_1$ and $e_y = \hat{y} - y$. To examine the stability of the error dynamics, the equivalent control is utilized as follows; first the output error e_y is guaranteed to reach zero value in finite time if v is selected as a discontinuous function of e_y

$$v = \tilde{A}_{22}e_y + \eta * sgn(e_y) \quad \dots (54)$$

where $sgn(e_y)$ is the signum function defined as follows;

$$sgn(e_y) = \begin{cases} 1 \text{ if } e_y > 0 \\ -1 \text{ if } e_y < 0 \end{cases} \quad \dots$$
(55)

and η is the discontinuous gain that must satisfy the following condition

$$\eta > |\tilde{A}_{21}e_1 - \tilde{D}_2\xi| \quad \dots (56)$$

If η satisfy the Inequality (56), then the sliding motion will ocuure on the sliding surface $e_y = 0$ after a finite time. By taking the initial condition for observer design as;

$$(\hat{x}_1, \hat{y})_{t=0} = (0, y(0)) \quad \dots (57)$$

and with v as in Eq. (49), we have $e_y = 0, \dot{e}_y = 0$ from the first instant i.e., $\forall t \geq 0$. The error dynamic stability based on the equivalent control is examined here as follows;

$$\begin{cases} \dot{e}_1 = \tilde{A}_{11}e_1 + \tilde{A}_{12}e_y - Lv - \tilde{D}_1\xi \\ \dot{e}_y = \tilde{A}_{21}e_1 + \tilde{A}_{22}e_y - v - \tilde{D}_2\xi \end{cases}_{eq} = $$
$$\begin{cases} \dot{e}_1 = \tilde{A}_{11}e_1 - Lv_{eq} - \tilde{D}_1\xi \\ 0 = \tilde{A}_{21}e_1 - v_{eq} - \tilde{D}_2\xi \end{cases},$$

which yields

$$\begin{cases} \dot{e}_1 = \tilde{A}_{11}e_1 + \tilde{A}_{12}e_y - Lv - \tilde{D}_1\xi \\ \dot{e}_y = \tilde{A}_{21}e_1 + \tilde{A}_{22}e_y - v - \tilde{D}_2\xi \end{cases}_{eq} = $$
$$\begin{cases} \dot{e}_1 = (\tilde{A}_{11} - L\tilde{A}_{21})e_1 + (L\tilde{D}_2 - \tilde{D}_1)\xi \\ v_{eq} = \tilde{A}_{21}e_1 - \tilde{D}_2\xi \end{cases}$$
$$\dots (58)$$

where v_{eq} is computed at $e_y = \dot{e}_y = 0$.

From Eq. (58) the unknown input term $(L\tilde{D}_2 - \tilde{D}_1)\xi$ in the estimation error dynamics will prevent the error e_1 from decaying

exponantionaly to zero where it represent the error source in the observation process. In fact, this term is the source of observer spillover that may cause instability in system response. Minimizing the error in the observation process is not an easy task but it influenced by the size of the reduced model and the selected L matrix.

6. Simulation Results and Discussion

The simulation results for a cantilever beam, which it subjected to an initial tip deflection, are presented in this section where the MATLAB software is used as a simulator to the cantilever beam system. The physical and geometrical specifications for the beam are given in Table (1) below.

Table 1: The physical and geometrical specification for the flexible cantilever beam and the piezoelectric

Physical Specification	Cantilever Beam (st-st 304L)	Piezoelectric
Length	L=300 mm	l_a =75 mm
Width	b =30 mm	b= 30 mm
Thickness	t_b =0.5 mm	t_a = 0.35 mm
Young modulus	E_b =193.06 Gpa	E_p = 68 Gpa
Density	ρ_b =8030 Kg/m^3	ρ_p = 7700 Kg/m^3
Damping coefficients	α = 0.001 & β = 0.0001	

Three steps are performed in the present work toward designing an active vibration control to the cantilever beam. In the first step, the natural frequencies for derived mathematical model of the beam (Eq. 47) are calculated and compared with the natural frequencies obtained from the ANSYS program. The results are found in Table (2) which show a good agreement. This proves that the derived model represent the system dynamics at least with respect to the dominant natural frequencies.

Also the balance realization and order reduction process for the system model had been performed to reduce its states form (16) state to (8) state, without affecting its dominant mode. Fig (2) shows the bode plot for the original system and balanced reduced system model with

dimension equal to eight and four. The figure clarify the matching between the original system and the reduced system of dimension (8) for the first four dominant modes.

Table 2: Natural frequency results of the system

Natural Frequency	MATLAB (Hz)	ANSYS (Hz)	Error%
f_1	4.4	4.399	0.022
f_2	27.609	27.57	0.141
f_3	77.814	77.202	0.792
f_4	153.5	151.3	1.45
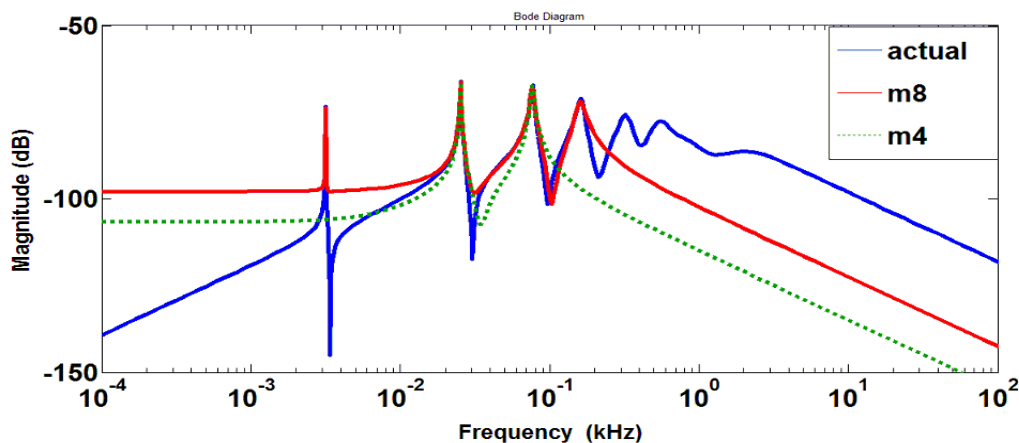
Figure 2: Bode plot for original system model and balanced reduced system model with 4 and 8 states

In the second step, the sliding mode observer is designed to the reduced order model. For the

reduced model of dimension eight, the estimated output using the SMO states ($y = C_r x_r$, x_r is the

estimated eight states) is compared with actual output in Fig. (3). Due to the discontinuous term injected in the SMO (v in Eq. (54) with $\eta = 500$)), the estimated output is chatters around the actual piezoelectric output. This is more clarified in Fig. (4) where the error between the actual output and the estimated output (Eqs. (47) & (52)) is plotted. The chattering effect, which will lead to inaccurate states estimation, can be removed by replacing the *signum* function (Eq. (55)) with a continuous approximate function. This function, among many approximations to the signum function [34], is the arc tan function;

$$sgn(e_y) \approx \frac{2}{\pi} * \tan^{-1}(n * e_y), \quad n = 0.01$$

Replacing $sgn(e_y)$ by the approximation given above will prevent chattering and smoothing the values of the estimated states Figs (5) and (6).

By using the estimated states, the designed control law based on the LQR approach is applied to the cantilever beam dynamic and the system is simulated for 10 mm initial tip displacement. Depending on the reduced order model dimension that selected according to the singular values, the LQR controller is designed accordingly and the new system eigenvalues are found in Table (3). Table (4) shows that by using reduced model of dimension two, four or six that can be selected according to the singular values, the control LQR does not change the value of the minimum absolute eigenvalue. But a good vibration damping and change in the value of the absolute minimum eigenvalue can be obtained when using the reduce model of dimension eight. Additionally, with the reduce model of dimension ten, the increase in the value of the minimum absolute eigenvalue is less than that the case of dimension eight. So the best choice of the reduce model dimension is eight.

The first set of numerical simulation to the control system and the SMO uses a 0.0001 second as a period of integration and with the approximate signum function in the observer design as defined above. In Fig. (7) the controlled tip displacement with the actual system output is compared, where, as shown, the amplitude is reduced to 80.6 % with respect to open loop after 15 second. In addition, the control input voltage to the piezoelectric element is plotted in Fig. (8), where, as can be seen, the control input started after 2 second. This delay in applying the control voltage is to prevent a high voltage required when it is computed from the first instant. This comes from the inaccuracies in states estimation during a small period after initiation. Also from Fig. (8) it can be seen that the maximum voltage does not exceed 30 volt which it is a direct consequence of using optimal control approach in designing u.
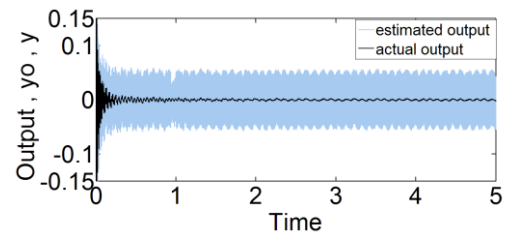
Figure 3: The actual piezoelectric output and the estimated output
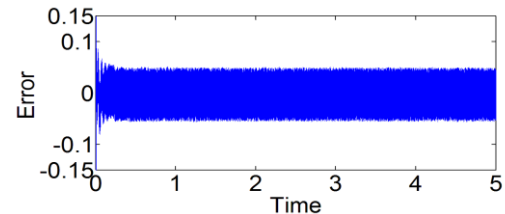
Figure 4: The error between the actual and the estimated output
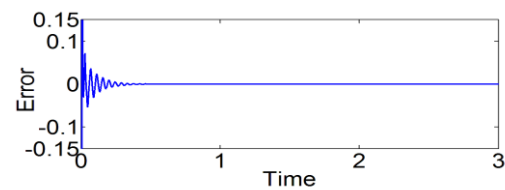
Figure 5: The error between the actual output and the estimated output (with removed chattering)
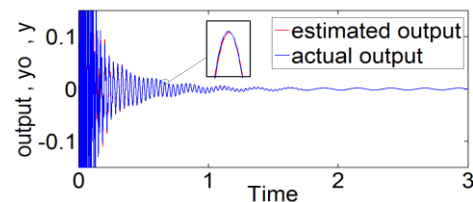
Figure 6: The actual piezoelectric output and the SMO output (with removed chattering)
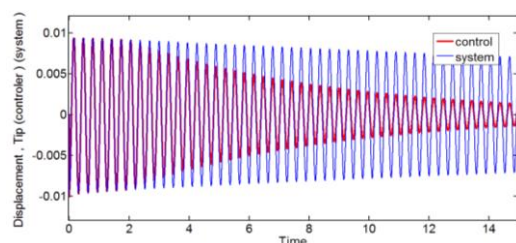
Figure 7: Tip Displacement for open loop and closed loop control system
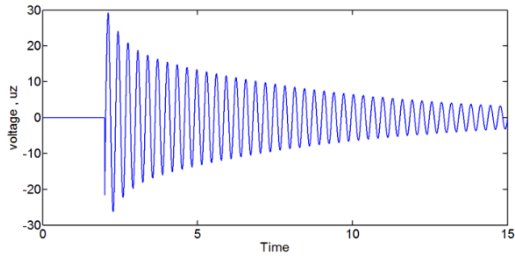
Figure 8: The control input voltage to the piezoelectric

Table 3: System eigenvalues and controlled system eigenvalues

System Eigenvalues	New System Eigenvalues
-69.181 +1003.5i	-69.379 + 1003.5i
-69.181 - 1003.5i	-69.379 - 1003.5i
-13.479 + 482.54i	-13.794 + 482.54i
-13.479 - 482.54i	-13.794 - 482.54i
-1.4057 + 159.21i	-1.4767 + 159.21i
-1.4057 - 159.21i	-1.4767 - 159.21i
-0.022488 + 19.886i	-0.27042 + 19.886i
-0.022488 - 19.886i	-0.27042 - 19.886i

Table 4: Minimum absolute eigenvalues for open and closed loop

Reduced Model Dimension	R	Q	Minimum Absolute Real Eigenvalue R^O (Open Loop)	Minimum Absolute Real Eigenvalue R^C (Closed Loop)	Maximum Control Input Voltage
2	1	300*diag [5 5]		0.02073	0
4	1	300*diag [1 1 2 2]		0.02073	0
6	1	300*diag [1 1 5 5 4 4]	0.022488	0.02073	0
8	1	300*diag [1 1 5 5 5 5 40 40]		0.27042	30
10	1	300*diag [1 1 5 5 5 5 40 40 5 5]		0.2245	28.5

In real application of the proposed controller it may be difficult to use 0.0001 second as a time period for the observer simulation that estimate the states after each such time period and for the control input where it is required to change the control voltage after each 0.0001 second. In order to approach the real situation, the time period for the observer is taken equal to 0.001 second (i.e., the change in the estimated eight states happened after each 0.001 second), while 0.025 second is the chosen time period where the control input changes. Consequently the second set of numerical simulation is based on these time numerical values for both; the observer simulation period of time and for the time period required for the control input voltage to change while the time period for the control system simulation is still equal to 0.0001 second. Fig. (9) plots the actual output and the estimated output with time. The effectiveness of the SMO can be detected from this figure where the idea is to force the estimated output to follow the actual one in a short time. After that, the estimated states will be used in the control law (Eq. (43)) which will attenuate the beam vibration. The tip displacements of the open and closed loop are plotted with time in Fig. (10),

where the amplitude of oscillation is reduced greatly after 15 second to reaches about 80.4% with respect to the open loop system. Additionally, the control input voltage is shown in Fig. (11), where, as can be seen, the vibration suppression ability is nearly the same as in the first set of simulation. This enhances the applicability of the proposed controller.
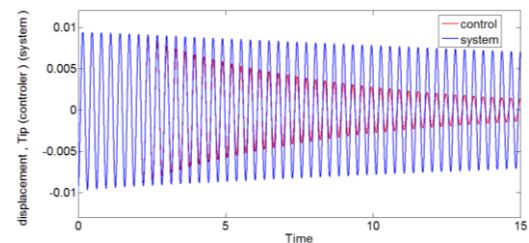
Figure 9: The actual piezoelectric output and the SMO output
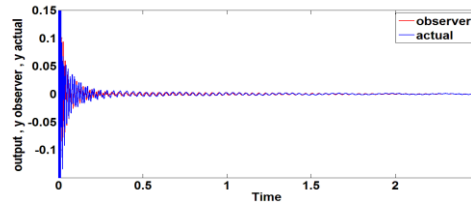
Figure 10: Tip Displacement for open loop and closed loop control system
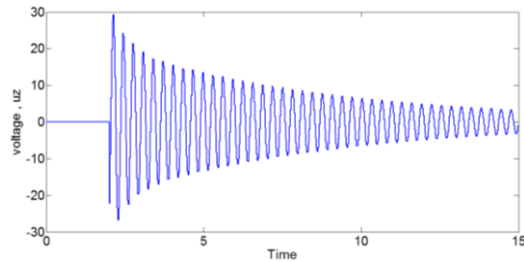
Figure 11: The control input voltage to the piezoelectric

7. Conclusions

In this paper, the state space model is obtained using the finite element approach and modal analysis resulting after appropriate modal reduction. During the theoretical calculations, the 16th order system model obtained from the finite element model is reduced to the 8th order using a model reduction technique based on balance realization without affecting its dominant modes.

As a basic requirement to the control design, the sliding mode observer is designed which estimates the eight states of the reduced model. In spite of the presence of the unknown inputs, which due to the residual model in the observer dynamics, the SMO forces the output, which is determined from the estimated states, to follow the actual output. This is taken place after approximately two second. After that, the reduced model states are estimated with bounded error.

To overcome the chattering problem in observer dynamics the *signum* function is replaced with the approximation given by the *arctan* function with appropriate parameters. The chattering is, consequently, prevented and the estimated states values are smoothened.

Using the estimated states, an LQR approach was designed based on the reduced order model. The control spillover was avoided by satisfying the avoidance condition where the minimum absolute real eigenvalue is 10 times that for the matrix *A* (**Table 4**). With the proposed LQR control and the SMO, the results show that for 10 mm initial tip displacement, the piezoelectric actuator reduce the tip displacement to about (1.3 mm) after 15 s.

References

[1]. M. U. S. Mehmet Itik, "Active Vibration Suppression of a Flexible Beam via Sliding Mode," *44th IEEE Conference on Decision and Control,* 2005.

[2]. J. Hu and Dachang Zhu, "Vibration Control of Smart Structure Using Sliding Mode Control with Observer," Journal Of Computers, vol. 7, 2012.

[3]. B. Bandyopadhyay, "Vibration Control of Smart Structure Using Second Order Sliding Mode Control," IEEE Conference on Control Applications, 2005.

[4]. S. Kumar, R. Srivastava and R.K.Srivastava, "Active Vibration Control Of Smart Piezo Cantilever Beam Using Pid Controller," International Journal of Research in Engineering and Technology, vol. 3, no. 1, 2014.

[5]. G. Sachs, "Intrinsic Dynamic Analysis And Control Design," USA, 2014.

[6]. D. J. Inman, Vibration with Control, USA: John Wiley & Sons Ltd, 2006.

[7]. B. C. Moor, "Principal Component Analysis in Linear Systems: Controllability, Observability, and Model Reduction," Transactions On Automatic Control. , Vols. AC-26, no. 1, 1981.

[8]. K. ZHOU and G. SALOMON, "Balanced Realization And Model Reduction For Unstable Systems," International Journal Of Robust And Nonlinear Control, vol. 9, pp. 183-198, 1999.

[9]. 9 L. MEIROVITCH, Dynamics and Control of Structures, USA: JOHN WILEY & SONS, 1990.

[10]. X. Dong, Z. Peng and W. Zhang, "Research on Spillover Effects for Vibration Control of Piezoelectric Smart Structures by ANSYS," Mathematical Problems in Engineering, 2014.

[11]. R. C. Dorf, optimal control system, New York: CRC Press LLC, 2003.

[12]. Oveisi and T. Nestorović, "Robust Mixed H_2/H_∞Active Vibration Controller In Attenuation Of Smart Beam," Mechanical Engineering , vol. 12, no. 3, pp. 235-249, 2014.

[13]. V. Utkin, Sliding Mode Control in Electro-Mechanical Systems, New York: Taylor & Francis Group, 2009.

[14]. H. Ko, K. Lee and H. Kim, "An intelligent based LQR controller design to power system stabilization," Electric Power Systems Research , vol. 71, pp. 1-9, 2004.

[15]. Alavinasab and H. Moharrami, "Active Control of Structures Using Energy-Based LQR Method," Computer-Aided Civil and Infrastructure Engineering, vol. 21, pp. 605-611, 2006.

[16]. A.J. ERICSSON and P. M. B~ah'tna, "The Optimal LQR Digital Control Of A Free-Free Orbiting Platform," Acta Astronautica, vol. 29, no. 2, pp. 69-81, 1993.

[17]. U. Aldemir, M. Bakioglu and S. S. Akhiev, "Optimal control of linear buildings under seismic excitations," Earthquake Engineering And Structural Dynamics, vol. 30, pp. 835-851, 2001.

[18]. D. G. LUENBERGER, "An Introduction to Observers," IEEE TRANSACTIONS ON MJTOMATIC CONTROL, vol. 16, no. 6, 1971.

[19]. V.I.Utkin and J.-X. Xu, "Vss Qbserver For Linear Time Varying System," IEEE, 1990.

[20]. B. L. WALCOT and STANISLAW H. ZAK, "Combined Observer- Controller Synthesis for Uncertain Dynamical Systems with Applications," *IEEE Transactions On Systems,* vol. 18, no. 1, 1988.

[21]. R. A. and S. H. Zak, "Variable Structure Control of Nonlinear Multivariable Systems," IEEE, vol. 76, no. 3, pp. 212-232, 1988.

[22]. C. Edwards, S. K. Spurgeon and R. J. Patton, "Sliding mode observers for fault detection and isolation," Automatica, vol. 36, pp. 541-553, 2000.

[23]. J.J.E.Slotion, "On Sliding Observers For Nonlinear System," Dynamic System, Mechanical and control, vol. 109, pp. 245-252, 1987.

[24]. J. L. S. H. Karanjit Kalsi, "Sliding-mode observers for systems with unknown inputs:

A high-gain approach," Automatica, vol. 46, 2010.

[25]. B. Bandyopadhyay, Modeling, Control and Implementation of Smart Structures, Springer Verlag Berlin Heidelberg, 2007.

[26]. D. Chhabra and K. Narwal, "Design and Analysis of Piezoelectric Smart Beam for Active Vibration Control," International Journal of Advancements in Research & Technology, vol. 1, no. 1, 2012.

[27]. N. Jalili, Piezoelectric-Based Vibration Control, USA: Springer Science+Business Media, LLC, 2010.

[28]. V. Balamurugan and S. Narayanan, "Active Vibration Control of Piezolaminated Smart Beams," 2000.

[29]. R. W. Clough, Dynamics Of Structures, USA: Computers & Structures, Inc., 2003.

[30]. R. L. Williams and D. A. Lawrence, Linear State-Space Control Systems, USA: JOHN WILEY & SONS, INC., 2007.

[31]. D. Janardhanan, Model Order Reduction and Controller Design Techniques.

[32]. J. B. Moor, Optimal Control linear qardatic methods, USA: prentice- hall, 1989.

[33]. S. Dhahri, "Robust sliding mode observer design for a class of uncertain linear systems with fault reconstruction synthesis," International Journal of Physical Sciences Vol. 7(8), pp. 1259 - 1269, 2012.

[34]. Edwards and S. K. Spurgeon. Sliding Mode Control: Theory and Applications. Taylor & Francis, 1998.

Appendix A: Derivation of Beam Mass and Stiffness Matrices

Consider the derivative of $w(x)$, which given in Eq. (1), as:

$$\frac{\partial w}{\partial x} = a_2 + 2a_3 x + 3a_4 x^2 \qquad (A1)$$

then at $x = 0$, $w(x) = a_1 = w_1$ and $\frac{\partial w}{\partial x} = a_2 = \theta_1$. Also at $x = l$,

$w(x) = w_2 = a_1 + a_2 l + a_3 l^2 + a_4 l^3$,

and, $\frac{\partial w}{\partial x} = \theta_2 = a_2 + 2a_3 l + 3a_4 l^2$

where $w_1, \theta_1, w_2,$ and θ_2 are Degree of Freedom at node 1 and 2, respectively and l is the length of the regular beam. The relation between $w_1, \theta_1, w_2, \theta_2$ and the constants a_1 to a_4 be represented in a matrix form as,

$$\begin{bmatrix} w_1 \\ \theta_1 \\ w_2 \\ \theta_2 \end{bmatrix} = \begin{bmatrix} 1 & 0 & 0 & 0 \\ 0 & 1 & 0 & 0 \\ 1 & l & l^2 & l^3 \\ 0 & 1 & 2l & 3l^2 \end{bmatrix} \begin{bmatrix} a_1 \\ a_2 \\ a_3 \\ a_4 \end{bmatrix} \qquad (A2)$$

Solving for a_1 to a_4 yields;

$$\begin{bmatrix} a_1 \\ a_2 \\ a_3 \\ a_4 \end{bmatrix} = \begin{bmatrix} 1 & 0 & 0 & 0 \\ 0 & 1 & 0 & 0 \\ -\frac{3}{l^2} & -\frac{2}{l} & \frac{3}{l^2} & -\frac{1}{l} \\ \frac{2}{l^3} & \frac{1}{l^2} & -\frac{2}{l^3} & \frac{1}{l^2} \end{bmatrix} \begin{bmatrix} w_1 \\ \theta_1 \\ w_2 \\ \theta_2 \end{bmatrix} \quad \text{Or,} \quad \begin{bmatrix} a_1 \\ a_2 \\ a_3 \\ a_4 \end{bmatrix} = \frac{1}{l^3} \begin{bmatrix} l^3 & 0 & 0 & 0 \\ 0 & l^3 & 0 & 0 \\ -3l & -2l^2 & 3l & -l^2 \\ 2 & l & -2 & l \end{bmatrix} \begin{bmatrix} w_1 \\ \theta_1 \\ w_2 \\ \theta_2 \end{bmatrix} \qquad (A3)$$

Substituting the constants obtained from Eq. (A3) into (2) and by rearranging the terms, the final form for $w(x)$ is obtained as:

$$w\,(x) = \frac{1}{l^3}\,[\,(\,l^3 - 3lx^2 + 2x^3)\ (\,l^3x - 2l^2x^2 + x^3l)\ (-l^2x^2 + lx^3\,)]\begin{bmatrix} w_1 \\ \theta_1 \\ w_2 \\ \theta_2 \end{bmatrix} \quad \text{(A4)}$$

Or $w\,(x) = N^T\,q$ (A5)

where N is the shape function and q is the displacements at the nodes, which are given by

$$N = \frac{1}{l^3}\,[\,(\,l^3 - 3lx^2 + 2x^3)\ (\,l^3x - 2l^2x^2 + x^3l)\ (-l^2x^2 + lx^3\,)]^T \quad \text{(A6)}$$

$q = [\,w_1\ \theta_1\ w_2\ \theta_2\,]^T$ (A7)

The strain energy U and the kinetic energy T for the beam element with uniform cross section in bending is obtained as:

$$U = \frac{E_b\,I_b}{2}\int_{l_b}\left[\frac{\partial^2 w}{\partial x^2}\right]^2 dx \quad = \frac{E_b I_b}{2}\int_{l_b}[w''\,(x\,,t\,)]^{\,T}\ [w''(x\,,t\,)]\,dx \quad \text{(A8)}$$

$$T = \frac{\rho_b A_b}{2}\int_{l_b}\left[\frac{\partial\,w}{\partial t}\right]^2 dx \quad = \frac{\rho_b A_b}{2}\int_{l_b}[\dot{w}\,(x\,,t\,)]^{\,T}\ [\dot{w}(x\,,t\,)]\,dx \quad \text{(A9)}$$

where ρ_b is the mass density of the beam material, A_b is the cross sectional area of the beam, I_b is the moment of inertia of the beam, and E_b is the modulus of elasticity of the beam material. The equation of motion of the regular beam element is obtained by using the Lagrangian equation:

$$\frac{d}{dt}\left[\frac{\partial\,T}{\partial\dot{q}_i}\right] + \left[\frac{\partial\,U}{\partial q_i}\right] = [F_i] \quad \text{(A10)}$$

For free vibration $F_i = 0$. The kinetic energy T can be expressed in terms of the shape function N and q are

$$T = \frac{\rho_b A_b}{2}\int_{l_b}[N^T\,\dot{q}\,]^T[\,N^T\dot{q}\,]\,dx \qquad = \frac{\rho_b A_b}{2}\int_{l_b}\dot{q}^T N N^T\dot{q}\,dx$$

$$= \dot{q}^T\left(\frac{\rho_b A_b}{2}\int_{l_b} N N^T dx\,\right)\dot{q} = \frac{1}{2}\dot{q}^T\,M_b\dot{q} \quad \text{(A11)}$$

Accordingly we get

$$\frac{\partial\,T}{\partial\dot{q}_i} = M_b\dot{q} \quad\quad\quad\quad\quad\quad\quad\quad \text{(A12)}$$

$$\frac{d}{dt}\left[\frac{\partial\,T}{\partial\dot{q}_i}\right] = M_b\,\ddot{q} \quad\quad\quad\quad\quad\quad\quad \text{(A13)}$$

where M_b is the mass matrix of regular beam

$$M_b = \rho_b\,A_b\int_{l_b} N N^T dx = \frac{\rho_b A_b l_b}{420}\begin{bmatrix} 156 & 22l_b & 54 & -13l_b \\ 22l_b & 4l_b^2 & 13l_b & -3l_b^2 \\ 54 & 13l_b & 156 & -22l_b \\ -13l_b & -3l_b^2 & -22l_b & 4l_b^2 \end{bmatrix} \quad \text{(A14)}$$

Also for the strain energy,

$$U = \frac{E_b\,I_b}{2}\int_{l_b}[N_2^T\,q\,]^T\ [\,N_2^T\,q\,]\,dx = \frac{E_b\,I_b}{2}\int_{l_b} q^T\,N_2\,.\,N_2^T\,q\ dx$$

$$= q^T\left(\frac{E_b\,I_b}{2}\int_{l_b} N_2\,N_2^T\ dx\right)q$$

$$= \frac{1}{2}\ q^T\,K_b\,q \quad\quad\quad\quad\quad\quad \text{(A15)}$$

we obtain

$$\left[\frac{\partial\,U}{\partial q_i}\right] = K_b\,q \quad\quad\quad\quad\quad \text{(A16)}$$

$$K_b = \ E_b\,I_b\int_{l_b}\ N_2\,N_2^T\ dx = \frac{E_b\,I_b}{l_b^3}\begin{bmatrix} 12 & 6l_b & -12 & 6l_b \\ 6l_b & 4l_b^2 & -6l_b & 2l_b^2 \\ -12 & -6l_b & 12 & -6l_b \\ 6l_b & 2l_b^2 & -6l_b & 4l_b^2 \end{bmatrix} \quad \text{(A17)}$$

السيطرة على تخميد الإهتزاز لعتبة مرنة مع إستخدام المخمن ذو الشكل المنزلق

عماد عبد الحسين عبد الصاحب   **محسن نوري حمزة**   **شبلي احمد السامرائي**

الجامعة التكنولوجية   الجامعة التكنولوجية   الجامعة التكنولوجية

قسم الهندسة الميكانيكية   قسم الهندسة الميكانيكية   قسم هندسة السيطرة والنظم

الخلاصة :

في هذه الدراسة، تم تنفيذ إخماد الاهتزاز في الهياكل الذكية، باستخدام المواد الكهرضغطية. يتكون الهيكل الذكي من عتبة كجزء اساسي، ومن المواد الكهرضغطية الملصقة على سطح العتبة والتي تمثل المؤثرات والمتحسسات. هناك مصدران من عدم الاستقرار في العتبة، وهما تأثير تداعيات المخمن وتأثير تداعيات السيطرة الغير مباشرة، حيث تم الاخذ بنظر الاعتبار هذين المصدرين في التصميم الحالي لنظام السيطرة على أساس نموذج مخفض من النظام الأصلي.

لتصميم نظام تحكم والذي من شأنه تخفيف الاهتزاز، تم استخدام طريقة (Balance realization) لاختيار نموذج مخفض حيث يكون هذا النموذج اكثر قابلية على السيطرة والتخمين. تم اختيار ثمانية متغيرات حالة للنموذج المخفض عن النظام الأصلي.

ان نظام المخمن المنزلق، والذي يستند على المسيطر المكافئ، يهدف إلى تقدير ثمانية متغيرات حالة حيث إن الخطأ في التخميد محدد كما تم إثباته. باستخدام تخمين المتغيرات عن طريق المخمن المنزلق، تم تصميم وحدة تحكم LQR الأمثل من شأنها أن تخفف من اهتزاز العتبة الذكية وباستخدام العنصر الكهرضغطي. وللتغلب على مشكلة تأثير السيطرة غير المباشرة، تم اشتقاق شرط تحقيق الاستقرارية والذي يضمن استقرار المسيطر للتصميم المقترح والذي سيقلل الاهتزاز في العتبة.

باستخدام المحاكاة العددية تم اختبار قدرة نظام السيطرة المقترح لتقليل وتخميد الاهتزاز. تم ازاحة طرف العتبة 10 مم، حيث وجد بان المؤثرات (actuator) للمادة الكهرضغطية (piz) قادرة على تقليل الازاحة إلى حوالي 1.3 ملم بعد 15 ثانية، في حين أنه يساوي 7 ملم في الحالة الحرة. ومن خلال المحاكاة تبين، أيضا، أن نظام السيطرة الأمثل يتم تنفيذه مع الحد الأدنى من الجهد حيث ان المطلوب هو 30 فولت فقط من أصل 200 فولت وهو الحد الاعلى لتشغيل المادة الذكية (Piz).